CHARACTERIZATION OF THE BMP2-SPECIFIC REGENERATION WINDOW IN THE ADULT MOUSE MIDDLE PHALANX MODEL OF INDUCED BONE REGENERATION

An Undergraduate Research Scholars Thesis

by

STACY NUÑEZ[1], DANIA MUHAMMAD[2], and PATRICK HALL[1]

Submitted to the Undergraduate Research Scholars program at
Texas A&M University
in partial fulfillment of the requirements for the designation as an

UNDERGRADUATE RESEARCH SCHOLAR

Approved by Research Advisors: Dr. Lindsay A. Dawson
Dr. Ken Muneoka

May 2020

Major: Biomedical Engineering[1]
Biomedical Sciences[2]

TABLE OF CONTENTS

ABSTRACT

Characterization of the BMP2-specific Regeneration Window in the Adult Mouse Middle Phalanx Model of Induced Bone Regeneration

Stacy Nuñez[1], Dania Muhammad[2], and Patrick Hall[1]
Departments of Biomedical Engineering[1] and Veterinary Medicine and Biomedical Sciences[2]
Texas A&M University

Research Advisors: Dr. Lindsay A. Dawson and Dr. Ken Muneoka
Department of Veterinary Physiology and Pharmacology
Texas A&M University

Mammalian regeneration capabilities are amputation-level-dependent; amputations of the terminal phalanx (P3) initiate regeneration mediated by a blastema, while amputations transecting more proximal levels of the digit fail to regenerate, resulting in bone truncation at the amputation plane and soft tissue scarring. Therefore, what distinguishes limb bone regeneration from scar formation is the blastema, a transient population of proliferating cells that regenerate the missing structures. The adjacent bone, the middle phalanx (P2), is non-regenerative after amputation. P2 can be induced to regenerate after treatment with Bone Morphogenetic Protein 2 (BMP2), however, the bone regeneration response is dependent on the timeframe after injury in which BMP2 is applied. This timeframe is called the Regeneration Window (RW). Utilizing adult mice, our objective was to characterize a pro-regenerative wound environment that supports limb regeneration in mammals. Using immunohistochemistry, we compared the P2 RW at 9 days post amputation (9 DPA), and the P2 timeframe when the RW is closed (24 DPA), with the known regeneration-permissive characteristics of the 9 DPA P3 blastema. We report that both the 9 DPA P3 blastema and the 9 DPA P2 wound site share regeneration characteristics

such as an absence of vasculature, robust proliferation, and the presence of progenitor cells. Conversely, the 24 DPA P2 wound site, when the RW is closed, is characterized by the presence of vasculature, minor proliferation, and the maturation of progenitor cells. Taken together, the 9 DPA P3 blastema and the 9 DPA P2 wound site share the presence of progenitor cells that pattern the final bone structure; however, while P3 progenitors are localized distal to the amputation plane and therefore result in a patterned regenerate, the P2 progenitors, in contrast, are circumferentially located and thus the wound site lacks the appropriate cues to pattern a regenerative response.

ACKNOWLEDGMENTS

We would like to thank the Veterinary Physiology and Pharmacology Department. Additionally, we would like to draw attention to the support we received from Dr. Ken Muneoka, Dr. Lindsay Dawson, Dr. Regina Brunauer, Dr. Ling Yu, Osama Qureshi, Katherine Zimmel, Mingquan Yan, and Ray Lin, for their guidance and support throughout the course of this research. The research was funded by Texas A&M University.

NOMENCLATURE

P3	Terminal Phalanx
P2	Middle Phalanx
BMP2	Bone Morphogenetic Protein 2
RW	Regeneration Window
DPA	Days Post Amputation
OSX	Osterix (Transcription Factor Sp7)
Runx2	Runt-Related Transcription Factor 2
Sox9	SRY- Box 9 Transcription Factor
PCNA	Proliferating Cell Nuclear Antigen
CXCR4	C-X-C Chemokine Receptor Type 4
EMCN	Endomucin
vWF 8	von Willebrand Factor 8
m	Marrow
c callus	Cartilaginous Callus
b callus	Bony Callus
bl	Blastema
DAPI	4’,6-Diamidino-2-Phenylindole, Dihydrochloride
EOC	Endochondral Ossification Center

CHAPTER I

INTRODUCTION

There are an estimated 2 million people in the United States living with limb loss [1]. Many opt for treatment involving the use of prosthetics or assistive devices. However, these treatments can be expensive, are often underutilized, and full restoration of function is almost never realized. Over the course of five years, costs associated with upper limb loss range from $31,129 to $117,440, and these costs will be significantly higher for people with lower limb loss who will pay $82,251 to $228,665 [2]. An alternative approach to prosthetics is to investigate how to target and enhance endogenous repair capabilities in mammals to induce regenerative responses. While humans and other mammals have the capacity to regenerate amputations of the distal tip of the finger, also known as the terminal phalanx (P3) without surgical intervention, [3–5] mammals do not have the regenerative capabilities to regrow entire limbs. This is in contrast to amphibians, such as axolotls, who have the ability to fully reform missing structures [6]. Amphibian regeneration follows an epimorphic pathway, i.e. regeneration mediated by the formation of a blastema, and the most studied mammalian model of epimorphic regeneration is the P3 distal amputation in adult mice. The blastema is defined as a population of proliferating cells that restores structures damaged by a traumatic injury and thus the blastema is an integral structure required for an epimorphic response to occur [6]. Epimorphic regeneration is a type of reparative regeneration; reparative regeneration is the biological response to an injury that results in restoration of form and function, and is delineated into i) epimorphosis, ii) tissue-specific regeneration not mediated by a blastema, such as fracture healing, and iii) cellular regeneration, defined as the reconstitution of a single cell [6].

Regeneration of the P3 digit is mediated by a specialized structure called the blastema which is comprised of a mass of proliferating cells that completely regrows the morphology of the amputated tissue resulting in a regenerate similar to the original structure [7–10]. P3 regeneration is mediated by intramembranous ossification, i.e. direct bone formation without a cartilaginous intermediate stage [8–10]. P3 regeneration is dependent on the amputation level, with more proximal amputations unable to elicit a regenerative response, leading to bone truncation and scar tissue [7, 8]. For example, when amputations are performed in the proximally adjacent middle phalanx (P2), a regenerative response is not observed. However, this does not mean that the injury site is inert. Instead, a dynamic bone healing process is initiated beginning with inflammation, periosteum-derived cartilaginous callus formation, and subsequent bone mineralization and remodeling [7]. This process, particularly cartilaginous callus formation, relies on the presence of the periosteum, a cellular layer that encircles the bone and directly contributes to the injury response [7, 11] and has also been implicated in the lineage of blastemal cells in regenerative P3 amputations [10].

Despite its proximal (non-regenerating) location, the P2 digit scarring injury response can be transformed into a regenerative response by the application of Bone Morphogenetic Protein 2 (BMP2); however, even this induced regenerative response only occurs when the cartilaginous callus is present, and is also temporally dependent on the maturation of periosteum-derived cells, indicating that there is a time frame of cellular responsiveness to BMP2 treatment called a "Regeneration Window", which corresponds to 9 days post amputation (DPA) [11]. When the periosteal callus matures to a bony callus, at 24 DPA, the wound site is no longer responsive to BMP2 treatment, thus the "Regeneration Window" is essentially closed [11]. Importantly, the "Regeneration Window" is not permanently closed after wound maturation, it can be reopened

with targeted periosteal re-injury, which induces another round of periosteal cartilaginous callus formation that is once again responsive to BMP2 treatment [11]. Intriguingly, the timing of the P2 “Regeneration Window” also corresponds to the P3 blastema stage; in other words, the P3 blastema is prominent at 9 DPA [10].

By characterizing the cellular environment of the Regeneration Window in non-regenerating P2 amputations and comparing it to the regenerating P3 amputations of the same time point as well as later stage (24 DPA) P2 amputations (when the Regeneration Window is closed), our aim was to identify shared cellular and molecular characteristics that are permissive for a regeneration response.

CHAPTER II

MATERIALS AND METHODS

A technician performed all surgical procedures on animals. A selection of 8-week-old female mice purchased from the Texas A&M Institute for Genomic Medicine (TIGM) were exposed to the anesthetic agent, isoflurane, in a controlled environment until unconscious. Following all protocols, mice toes were amputated either at the second phalanx (P2) or the third distal phalanx (P3). P3 amputation transects the nail, the underlying dermis and bone, but does not transect the marrow cavity [10]. P2 amputation bisects the P2 bone, and completely removes the P3 bone and nail [7]. Digits were then collected at 9- and 24-days post amputation (DPA) and were provided to the students. After collection, the digits were fixed in Zinc Formalin Fixative (Z-Fix, Anatech Ltd., Battle Creek, MI; 24–48 hours) and then decalcified by Surgipath's Decalcifier I (Surgipath, Leica Biosystems, Richmond, IL; overnight). Digits were processed for paraffin infiltration and embedded in paraffin wax. Digit sections were created with a microtome at 4.5 micrometers and affixed onto glass slides.

Histology and Immunohistochemistry

Mallory Trichrome histological staining was used to visualize the morphology of the tissue.

Immunohistochemical staining was performed to identify the presence of the cartilage marker SRY Box-9 (SOX 9, 1:500 concentration); osteogenic markers Runt related transcription factor 2 (RUNX2, 1:250 concentration) and Osterix (OSX, 1:400 concentration); blastemal markers C-X-C chemokine receptor 4 (CXCR4, 1:500 concentration), proliferating cell nuclear antigen (PCNA, 1:1000 concentration); and the endothelial cell markers Endomucin (EMCN,

1:73 concentration), and von Willebrand factor 8 (vWF 8, 1:800 concentration). The process of immunostaining was started by deparaffinizing and washing samples briefly with Tris-buffered saline with Tween 20 (TBST, Sigma–Aldrich Co., St Louis, MO). Antigen retrieval was performed using either of two methods. The first method was an enzymatic retrieval using Proteinase-K (DAKO, Carpinteria, CA; 10 mg/mL, 37 C, 15 minutes). The second method was a heat retrieval protocol using either citrate buffer of pH 6 (Invitrogen, Carlsbad CA, 90 °C, 25 minutes) or ethylenediaminetetraacetic acid (EDTA) buffer with a pH of 8 (Thermo Fisher Scientific, Waltham, MA, 90 °C, 25 minutes). Next, after a gradual cooling process, protein block (DAKO, 1 hour, room temperature) was applied, and the slides were left in a humidifying chamber. PCNA, Runx2, and EMCN immunostaining were performed using EDTA heat retrieval, monoclonal mouse anti-PCNA antibody (Abcam, Cambridge, UK; ab29, 1:1000), and Alexa Fluor 647 Goat anti-mouse IgG secondary antibody (Invitrogen; A21235, 1:500), rabbit anti-Runx2 antibody (Sigma–Aldrich Co., HPA022040; 1:250) with Alexa Fluor goat anti-rabbit 488 IgG secondary antibody (Invitrogen; A11008, 1:500), EMCN (Abcam; 1:73) with Alexa Fluor 488 goat anti-rat IgG secondary antibody (Invitrogen; A-11006, 1:500). CXCR4 and vWF 8 immunostaining was performed using proteinase K retrieval, rat anti-CXCR4 antibody (R&D Systems; MAB21651, 1:500 dilution) and Alexa Fluor 488 goat anti-rat IgG secondary antibody (Invitrogen; A-11006, 1:500), polyclonal rabbit anti-human vWF 8 antibody (DAKO; A0082, 1:800), and Alexa Fluor 568 goat anti-rabbit IgG secondary antibody (Invitrogen; A-11011, 1:500). The OSX immunostaining was performed using citrate heat retrieval, rabbit anti-OSX, SP7 monoclonal antibody (Abcam; ab22552, 1:400) and the Alexa Fluor goat anti-rabbit 488 IgG secondary antibody (Invitrogen; A11008, 1:500). The SOX-9 immunostaining was performed using citrate heat retrieval, rabbit anti-Sox9 monoclonal antibody (Abcam; ab185966,

1:500) and the Alexa Fluor goat anti-rabbit 488 IgG secondary antibody (Invitrogen; A11008, 1:500).

The Olympus VS120 microscope was utilized to perform fluorescence microscopy on the immunohistochemistry stained samples and bright field microscopy for histological stained samples.

CHAPTER III

RESULTS

In order to study regenerative processes, a standard model is used which is the amputation of the P3 bone of the digit on the hind limb of a mouse (**Figure 1A**). This model follows 5 steps in the post amputation period: histolysis, wound closure, blastema formation, differentiation, and reformation [8–10]. Histolysis is the initial period after the amputation, in which bone is degraded to expose the marrow cavity to the wound mesenchyme, and an endogenous secondary amputation is formed. Next, the bone fragment from the secondary amputation is ejected, and the epidermis begins to seal the wound [9, 10]. At this point, the wound is closed, and the blastema is prominent [10]. The blastema is localized distal to the amputation plane, shown at 9 DPA (**Figure 1B**), and the regenerating digit shows evidence of new bone formation adjacent to the stump. The new bone is formed by osteoblasts through the process of direct intramembranous ossification and grows outwards proximal to distal [8–10]. In contrast, the P2 amputation model (**Figure 1A**, dashed line) is mediated by an endochondral callus, similar to fracture healing, rather than a blastema. The process is demarcated by a dynamic healing response characterized by the stages of inflammation, wound closure, cartilaginous callus formation prominent at 9 DPA (**Figure 1C,D**, outlined), woven bony callus formation, shown at 24 DPA (**Figure 1E**, outlined), and bone remodeling. After P2 amputation, this final structure is not equivalent to the original and is characterized by bone truncation as well as scar tissue formation.

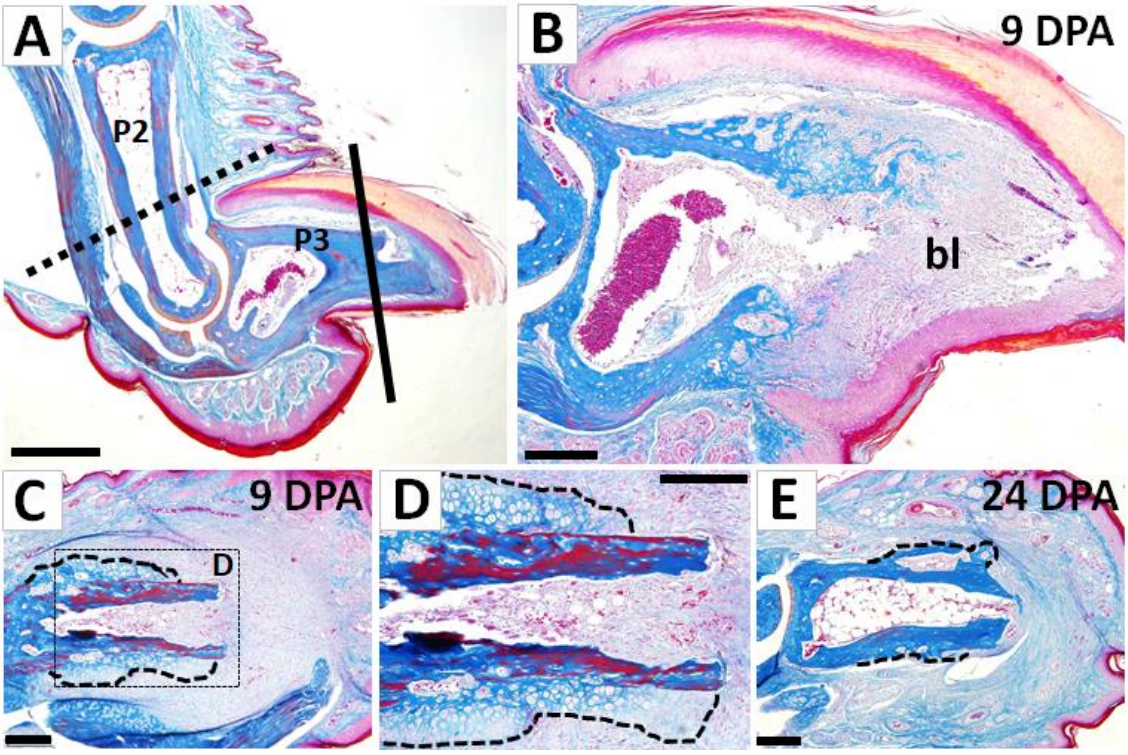

Figure 1: The Mallory-stained histological structures of a digit pre- and post-amputation. (A) The amputation planes for both P2 (dashed line) and P3 (solid line). (B) The 9 DPA P3 digit is characterized by a blastema distal to the amputation plane. (C) The 9 DPA P2 digit is characterized by cartilaginous callus formation (outlined) along the stump. (D) High-mag image of the cartilaginous callus (outlined). (E) At 24 DPA, the cartilaginous callus is no longer present and the P2 stump is characterized by the woven bony callus (outlined). Scale bars: (A) 500 µm; (B)-(E): 100 µm. Distal is to the right, dorsal is to the top.

The Regeneration Window Exhibits Blastemal Characteristics

Immunohistochemical analysis was performed to investigate potential similarities because the 9 DPA P3 blastema and the 9 DPA P2 wound corresponding to the "Regeneration Window", as well as the 24 DPA P2 wound when the "Regeneration Window" is closed. Our analysis included probing for these 7 markers: PCNA, CXCR4, EMCN, vWF 8, Runx2, Sox9, and OSX. The initial comparison between the models was focusing on identifying blastemal characteristics and their histological patterns. The blastema is characterized by cell proliferation, cell migration, and the lack of organized vasculature [8–10]. In order to assess for cell

proliferation, immunostaining was performed using Proliferating Cell Nuclear Antigen, (PCNA). In both the P3 blastema **(Figure 2A)** and 9 DPA P2 wound environment **(Figure 2A')**, robust PCNA expression is present, whilst in the 24 DPA P2 **(Figure 2A'')**, only minimal PCNA expression is observed. Immunostaining for the cell migration marker, C-X-C chemokine receptor type 4 (CXCR4), demonstrates uniform expression in both P2 samples **(Figure 2B', B'')** and localized expression in the blastema of the P3 sample **(Figure 2B)**. CXCR4 marks the migration ability of cells, and since all of the samples have similar robust expression, is a poor identifier for a pro-regenerative wound environment. Immunolabeling for Endomucin (EMCN), a marker for vasculature, indicates the presence of endothelial cells peripheral to the blastemal region of the P3 sample **(Figure 2C)**, as well as localized angiogenesis in the marrow cavity of the 9 DPA P2 **(Figure 2C')** and minor vasculature growth in the proximal region of the 24 DPA P2 marrow cavity **(Figure 2C'')**. Importantly, the 9 DPA P2 cartilaginous callus is not EMCN+ (**Figure 2C'**), whereas the 24 DPA P2 bony callus shows few EMCN+ cells (**Figure 2C''**). Immunostaining for von Willebrand Factor 8, an endothelial cell marker, is associated with the periphery of the P3 blastema **(Figure 2D)**, as well as the digit apex of the 9 DPA P2 but not the cartilaginous callus **(Figure 2D'),** and is present in the bony callus of the 24 DPA P2 digit **(Figure 2D'')**. These immunohistochemical findings identify shared similarities between the 9 DPA P3 blastema and the 9 DPA P2 cartilaginous callus; the presence of proliferating cells and the absence of organized vasculature.

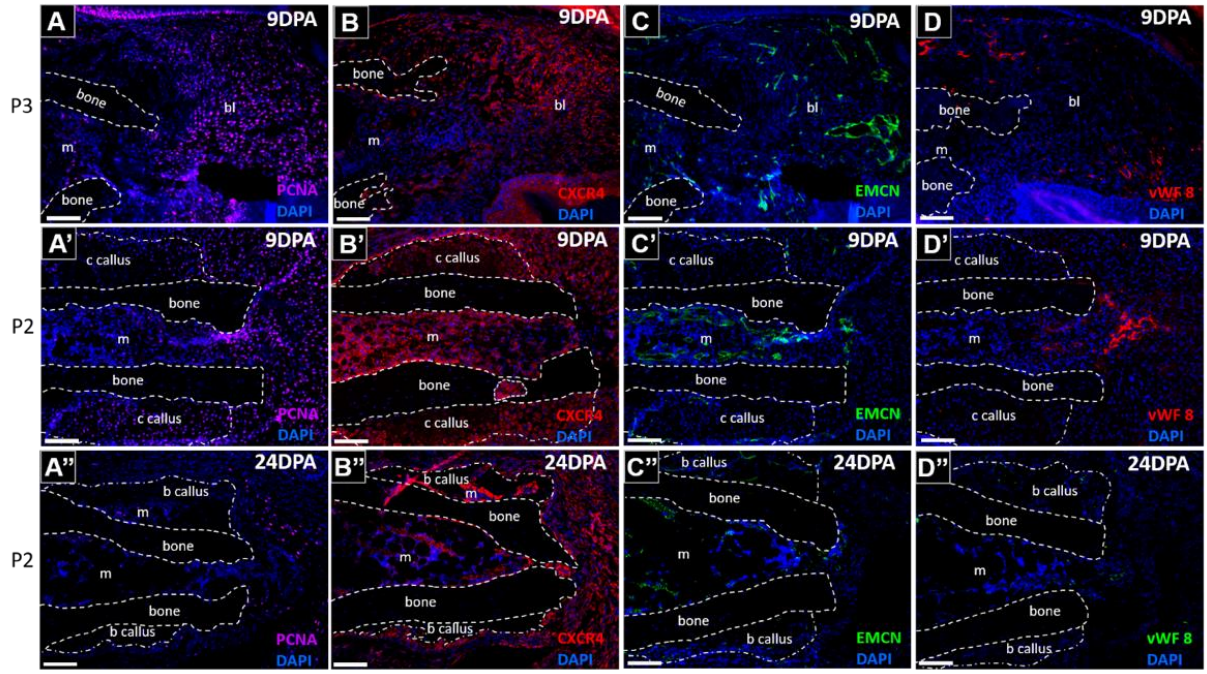

Figure 2: The Regeneration Window exhibits blastemal characteristics. (A-A'') Immunostaining for PCNA. (A) The 9 DPA P3 digit shows PCNA expression localized to the blastema. (A') The 9 DPA P2 digit demonstrates PCNA expression distal to the bone stump and within the c callus. (A'') The 24 DPA P2 digit shows sparse PCNA expression predominantly localized distal to the bone, as well as within the marrow cavity of the b callus. (B-B'') Immunostaining for CXCR4. (B) The 9 DPA P3 digit demonstrates robust CXCR4 expression localized to the blastema. (B') The 9 DPA P2 digit exhibits uniform CXCR4 expression throughout the digit. (B") The 24 DPA P2 digit shows CXCR4 expression throughout the b callus and distal to the bone. (C-C'') Immunostaining for EMCN. (C) The 9 DPA P3 digit expresses EMCN distal to the blastemal region. (C') The 9 DPA P2 digit expresses EMCN within the marrow cavity. (C'') The 24 DPA P2 digit tests immunopositive for EMCN localized to the proximal section of the P2 marrow cavity. (D-D'') Immunostaining for vWF 8. (D) The 9 DPA P3 digit demonstrates vWF 8 expression dorsal to the bone as well as distal to the blastema. (D') The 9 DPA P2 digit tests immunopositive for vWF 8 expression directly distal to the bone. (D'') The 24 DPA P2 digit exhibits vWF 8 within the b callus. Immunohistochemically stained samples are counterstained with DAPI. Dorsal is to the top, and distal is to the right. M, marrow; bl, blastema; c callus, cartilaginous callus; b callus, bony callus. All scale bars are 100 um.

The Blastema and the Regeneration Window are Comprised of Progenitor Cells

To investigate bone and cartilage regeneration after amputation, we performed immunohistochemistry for osteoprogenitors, osteoblasts, and chondroprogenitors. Immunostaining for Runt related transcription factor 2 (Runx2), an osteoprogenitor marker,

showed robust expression in the P3 blastema **(Figure 3A)**, as well as broad expression in the 9 DPA P2 digit within the marrow cavity and the cartilaginous callus **(Figure 3A')**, and minimal expression in the 24 DPA P2 digit localized to the bony callus **(Figure 3A'')**. To assess for chondrogenesis, staining for the early chondrogenic marker SRY-Box Transcription Factor 9 (Sox9) was performed. In the P3 blastema **(Figure 3B)**, limited expression is present, while in the 9 DPA P2 digit **(Figure 3B')**, broad expression is localized to the cartilaginous callus, and no expression is observed in the 24 DPA P2 digit **(Figure 3B'')**. Immunolabeling for Osterix (OSX), an osteoblast marker, was conducted and OSX expression is limited to the proximal region of the P3 wound site, associated with new bone regeneration, but is absent from the distal blastema **(Figure 3C)**. The 9 DPA P2 wound site demonstrates OSX immunostaining on the periphery of the cartilaginous callus **(Figure 3C'),** while the 24 DPA P2 wound site shows OSX immunostaining associated with the marrow region of the bony callus **(Figure 3C'')**. Taken together, both the 9 DPA P3 blastema and the 9 DPA P2 cartilaginous callus are comprised of progenitor cell populations, but the progenitor populations differ between the two wound sites, i.e. osteoprogenitors comprise the P3 blastema, whereas chondrogenitors are abundant within the P2 cartilaginous callus.

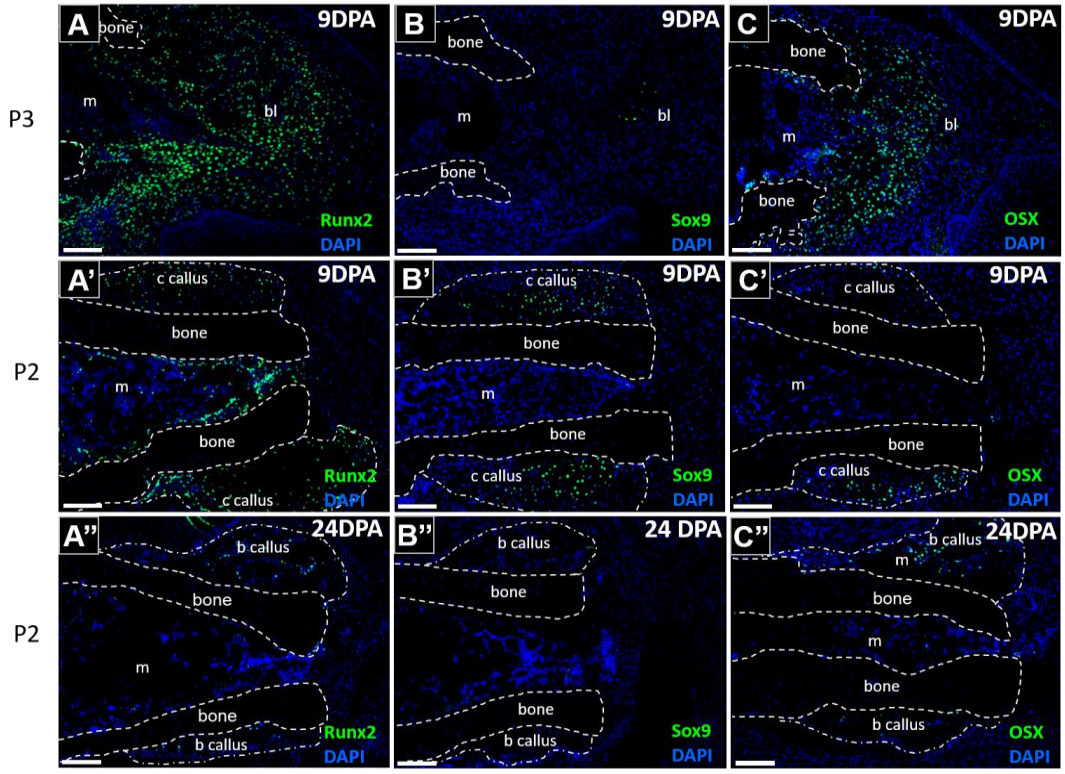

Figure 3: The P3 blastema and the P2 Regeneration Window is comprised of progenitor cells. (A-A") Immunostaining for Runx2. (A) The 9 DPA P3 digit shows Runx2 expression localized to the blastema. (A') The 9 DPA P2 digit demonstrates Runx2 expression both within the c callus and the marrow cavity. (A'') The 24 DPA P2 digit exhibits Runx2 expression localized to the b callus. (B-B'') Immunostaining for Sox9. (B) The 9 DPA P3 digit displays minimal Sox9 expression in the medial blastema. (B') The 9 DPA P2 digit exhibits robust Sox9 expression limited to the c callus region. (B'') The 24 DPA P2 digit does not express Sox9. (C-C'') Immunostaining for OSX. (C) The 9 DPA P3 digit shows OSX expression adjacent to the bone stump. (C') The 9 DPA P2 digit displays OSX expression in the c callus region. (C'') The 24 DPA P2 digit expresses OSX in the marrow cavity of the b callus. Immunohistochemically stained samples are counterstained with DAPI. Dorsal is to the top, and distal is to the right. M, marrow; bl, blastema; c callus, cartilaginous callus; b callus, bony callus. All scale bars are 100 um.

CHAPTER IV

CONCLUSION

The mammalian limb regeneration response is amputation level dependent; distal amputation of P3 initiates a robust regeneration response and restores form, whereas amputations proximal to the nail bed fail to mount a regeneration response [8]. The P3 model is an example of epimorphic regeneration, i.e. regeneration mediated by the formation of a blastema [6, 8–10]. Importantly, formation of the P3 blastema and subsequent bone regeneration is dependent on Bone Morphogenetic Protein (BMP) signaling [12]. The blastema is a transient cell population of proliferating cells that function to restore missing structures [6, 8–10]. There are several blastemal characteristics that are required for successful P3 regeneration, including blastemal avascularity [13], SDF-1/CXCR4 signaling [14], progenitor cell contribution to the blastema [10], and blastemal cell proliferation [8–10].

Conversely, amputation of P2 does not initiate blastema formation, therefore P2 is a model to investigate regenerative failure and is a wound site to test strategies to enhance mammalian bone and joint regeneration [7, 11, 14]. Similar to limb amputation, amputation of P2 results in bone truncation and scar formation. Although P2 fails to regenerate, P2 undergoes a dynamic bone healing response that is characterized by inflammation, the presence of a cartilaginous callus by 9 DPA which ossifies into a woven bony callus that is evident by 24 DPA [7]. Previous research identified a time frame in which the P2 wound site can be induced to regenerate using bone morphogenetic protein 2 (BMP2), and this time frame corresponds to the cartilaginous callus phase of P2 bone healing [11]. The application of BMP2 functions to transition the scarring event into a robust regenerative response. This process is characterized by

the accumulation of proliferating chondrocytes that form a cartilaginous callus localized distal to the amputation plane that functions as a template for bone regeneration to restore the amputated bone length [11]. In other words, when BMP2 is administered at 9 DPA when the cartilaginous callus is prominent, a regeneration response occurs, however, treating the wound site at 24 DPA when the cartilaginous callus has been converted to a bony callus, no response is observed [11]. Importantly, when a 24 DPA digit is re-amputated and treated with BMP2 at nine days post re-injury, a regeneration response will occur [11]. Therefore, re-amputation of a previously healed bone injury can stimulate the formation of a cartilaginous callus that can once again be responsive to BMP2 treatment [11]. Taken together, as the P2 skeletal wound matures, BMP responsiveness is diminished, but can be reactivated through re-injury. The temporal window for BMP responsiveness is associated with the presence of the cartilaginous callus and is defined as the “Regeneration Window”.

We discovered that the P2 Regeneration Window and the P3 blastema have similar characteristics that are associated with a pro-regenerative wound environment. It is well established that for a P3 epimorphic regenerative response to occur, one of the variables needed is hypoxia and by extension; avascularity [13]. We report that both the 9 DPA P2 and the 9 DPA P3 wound sites have disorganized vasculature which implies the hypoxic environment needed to establish a pro-regeneration wound environment that supports bone regeneration. The second main characteristic of the P3 regenerative response that was assayed for was a robust population of proliferating cells. The immunostaining for Proliferating Cell Nuclear Antigen (PCNA) demonstrates that both P2 9 DPA and P3 9 DPA samples have large populations of proliferating cells localized to the wound site, including the cartilaginous callus, and the blastema, respectively. On the other hand, in 24 DPA P2 digits when the Regeneration Window is closed,

proliferation is not associated with the bone and the newly formed bone is vascularized. An important finding from our study is that C-X-C Chemokine receptor type 4 (CXCR4) is not an adequate marker that distinguishes a pro-regeneration wound environment from one that results in regenerative failure. Robust CXCR4 expression is observed in all three time points. Since CXCR4 expression is seen uniformly at all time points assayed, and is also a marker of cell migration, this suggests CXCR4 expression is not exclusive to a pro-regenerative wound environment.

We also discovered that the P2 Regeneration Window and the P3 blastema are both composed of progenitor cells associated with bone regeneration, yet the progenitor populations are different. For example, the P2 Regeneration Window is rich in Sox9+ chondroprogenitors, while the P3 blastema is comprised of osteoprogenitors. Conversely, the 24 DPA P2 digit consists of few progenitor cells, and since progenitor cells are required for successful P3 regeneration, this characteristic may be linked to the closure of the Regeneration Window. These findings suggest the presence of Sox9+ chondroprogenitor cells can aid in the identification of the Regeneration Window in amputated long bones.

Taken together, we report that the P2 Regeneration Window shares several characteristics with the P3 blastema that may trigger a pro-regeneration wound environment, including transient avascularity, cell proliferation, and the presence of a progenitor cell population that can contribute and/or coordinate the regeneration response.

REFERENCES

1. Ziegler-Graham K, MacKenzie EJ, Ephraim PL, Travison TG, Brookmeyer R. Estimating the Prevalence of Limb Loss in the United States: 2005 to 2050. Archives of Physical Medicine and Rehabilitation. 2008;89: 422–429. doi:10.1016/j.apmr.2007.11.005

2. Blough DK, Hubbard S, McFarland LV, Smith DG, Gambel JM, Reiber GE. Prosthetic cost projections for servicemembers with major limb loss from Vietnam and OIF/OEF. J Rehabil Res Dev. 2010;47: 387–402.

3. Illingworth CM. Trapped fingers and amputated finger tips in children. Journal of Pediatric Surgery. 1974;9: 853–858. doi:10.1016/S0022-3468(74)80220-4

4. Borgens R. Mice regrow the tips of their foretoes. Science. 1982;217: 747–750. doi:10.1126/science.7100922

5. Douglas BS. CONSERVATIVE MANAGEMENT OF GUILLOTINE AMPUTATION OF THE FINGER IN CHILDREN. J Paediatr Child Health. 1972;8: 86–89. doi:10.1111/j.1440-1754.1972.tb01793.x

6. Carlson BM, editor. Principles of regenerative biology. Amsterdam ; Burlington, Mass: Elsevier/Academic Press; 2007.

7. Dawson LA, Simkin J, Sauque M, Pela M, Palkowski T, Muneoka K. Analogous cellular contribution and healing mechanisms following digit amputation and phalangeal fracture in mice: Analogous Cellular Contribution and Healing Mechanisms. Regeneration. 2016;3: 39–51. doi:10.1002/reg2.51

8. Han M, Yang X, Lee J, Allan CH, Muneoka K. Development and regeneration of the neonatal digit tip in mice. Developmental Biology. 2008;315: 125–135. doi:10.1016/j.ydbio.2007.12.025

9. Fernando WA, Leininger E, Simkin J, Li N, Malcom CA, Sathyamoorthi S, et al. Wound healing and blastema formation in regenerating digit tips of adult mice. Developmental Biology. 2011;350: 301–310. doi:10.1016/j.ydbio.2010.11.035

10. Dawson LA, Schanes PP, Kim P, Imholt FM, Qureshi O, Dolan CP, et al. Blastema formation and periosteal ossification in the regenerating adult mouse digit: Ossification in the regenerating digit. Wound Rep and Reg. 2018;26: 263–273. doi:10.1111/wrr.12666

11. Dawson LA, Yu L, Yan M, Marrero L, Schanes PP, Dolan C, et al. The periosteal requirement and temporal dynamics of BMP2-induced middle phalanx regeneration in the adult mouse: Dawson et al. Regeneration. 2017;4: 140–150. doi:10.1002/reg2.81

12. Yu L, Han M, Yan M, Lee E-C, Lee J, Muneoka K. BMP signaling induces digit regeneration in neonatal mice. Development. 2010;137: 551–559. doi:10.1242/dev.042424

13. Yu L, Yan M, Simkin J, Ketcham PD, Leininger E, Han M, et al. Angiogenesis is inhibitory for mammalian digit regeneration: Angiogenesis Inhibits Regeneration. Regeneration. 2014;1: 33–46. doi:10.1002/reg2.24

14. Lee J, Marrero L, Yu L, Dawson LA, Muneoka K, Han M. SDF-1α/CXCR4 signaling mediates digit tip regeneration promoted by BMP-2. Developmental Biology. 2013;382: 98–109. doi:10.1016/j.ydbio.2013.07.020